COVID-19 in Austin, Texas: Averting healthcare surges while relaxing social distancing

Presented to the Austin City Council on April 28, 2020

The University of Texas COVID-19 Modeling Consortium
Contributors: Daniel Duque, David P. Morton, Bismark Singh, Zhanwei Du, Remy Pasco, Lauren Ancel Meyers
Contact: utpandemics@austin.utexas.edu

Overview

To support planning by the city of Austin and Travis County, we analyzed the Austin-Round Rock module of our *US COVID-19 Pandemic Model* to project the number of hospitalizations under different social distancing scenarios. Note that the results presented herein are based on multiple assumptions about the transmission rate and age-specific severity of COVID-19. There is still much we do not understand about the transmission dynamics of this virus, including the extent of asymptomatic infection and transmission. These results do not represent the full range of uncertainty. Rather, they are meant to serve as plausible scenarios for designing optimal triggers for enacting stricter social distancing measures in the Austin-Round Rock Metropolitan Area.

We have updated our model inputs based on the daily number of COVID-19 hospitalizations in the Austin-Round Rock MSA between March 13 and April 19, 2020. The data suggest that social distancing following the March 24th Stay Home-Work Safe order has resulted in a 94% reduction in COVID-19 transmission, with our uncertainty in this estimate ranging from 55% and 100%. The data also suggest that approximately 13.6% of symptomatic cases are detected (i.e., reported as confirmed cases).

We are posting these results prior to peer review to provide intuition for both policy makers and the public regarding both the immediate threat of COVID-19 and the extent to which early social distancing measures are mitigating that threat. Our projections indicate that the Stay Home-Work Safe has delayed and possibly even prevented a COVID-19 healthcare crisis in the region.

COVID-19 projections for the five-county Austin-Round Rock MSA with school closures and social distancing

We updated the Austin-Round Rock module of our *US COVID-19 Pandemic Model* to simulate COVID-19 epidemics under various assumptions about the efficacy of Austin's *Stay Home-Work Safe* order that was enacted on March 24, 2020.

The simulations ran from February 15 through mid-August, 2020 by assuming the following initial conditions and key parameters:

- Starting condition: February 15, 2020 with 1 infected adult
- Time course of interventions
    - February 15 - March 14, 2020: No interventions
    - March 15 - August 17, 2020: Schools closed [1]
    - March 25 - May 1, 2020: *Stay Home - Work Safe* reduces transmission by 95%
    - May 1, 2020 - September 30, 2020: Various scenarios for alternating between relaxation (40% reduction in transmission) and lock-down (90% reduction in transmission)
- $\beta = 0.035$ (based on fitting our model to daily COVID-19 hospitalizations in Austin-Round Rock MSA for March 13-April 5, 2020). This corresponds to an epidemic doubling time prior to school closures of 2.9 days
- Average incubation period (assuming 12.1% of transmission happens pre-symptomatically): 6.9 days [2]
- Proportion of cases asymptomatic (assumed 46% as infectious as symptomatic cases): 17.9% [3]

Figures 1 and 2 summarize results of COVID-19 analyses for the Austin-Round Rock MSA. The model structure and parameters, including age-specific hospitalization and fatality rates, are described in the Appendices below.

We project COVID-19 hospitalizations and deaths through September, 2021 under **four different scenarios**. In all cases, we assume that the Stay-Home Work Safe order reduces transmission by 95% until May 1, 2020. The model projects that the relaxation of social distancing measures beginning on May 1st would be expected to lead to a second pandemic wave, unless the Austin-Round Rock MSA population continues to take precautions that reduce the risk of transmission by over 80%.

Scenario 1: Austin continues to reduce transmission by 90% until September 30, 2021 (Figure 1, top) through a combination of vigilant social distancing, precautions to prevent transmission during contacts, voluntary and rapid self-isolation upon feeling symptoms, receiving a positive COVID-19 test result, or close contact with an infectious case, and aggressive testing, contact tracing and isolation of cases.

Scenario 2: Austin relaxes social distancing starting on May 1st and maintains only a 40% (rather than 90%) reduction in transmission until September 30, 2021 (Figure 1, bottom). In this case, the model projects a catastrophic surge in hospitalizations and deaths in late summer that far exceeds local healthcare capacity.

Scenario 3: Austin relaxes social distancing starting on May 1st, but follows an *optimized policy* for reinstating the Stay Home Work Safe lockdown and maintains 95% effective cocooning of high-risk populations, who make up roughly 25% of the total Austin-Round Rock MSA population (Figure 2, top).

The policy uses a trigger determined by monitoring two quantities:

- Initiate a lockdown when daily hospital admissions cross an optimized trigger value.
- Relax a lockdown when daily hospital admissions decline back below the trigger value AND total daily hospitalizations are below a *safety threshold* (a fixed proportion of total bed capacity).

We project that a second pandemic wave will emerge in early June 2020 and trigger a three-month lock down that ends in mid-September, after which schools can open. It further projects that a third pandemic wave will emerge in the fall and peak in December of 2020, without requiring any additional days of lock-down.

Scenario 4: Identical to scenario 3, except that cocooning is only 80% effective at reducing the risk of infection in vulnerable populations. Failing to fully cocoon high-risk populations dramatically increases the expected morbidity and mortality and requires nearly double the days of lock-down to prevent overwhelming hospital surges, relative

to scenario 3. Under this optimized scenario, schools would remain closed for much of the 2020-2021 academic year and over 6000 people would die.

Our projections highlight the **importance of cocooning vulnerable populations**, including older adults and individuals of all ages with underlying high risk conditions. Such measures would be expected to substantially reduce the numbers of COVID-19 hospitalizations and deaths during a future pandemic waves. Residents of long-term care facilities such as nursing homes are at particular risk. Measures to prevent COVID-19 introductions and rapidly contain cases in long-term care facilities are critical and may require substantial increases in staffing, limiting the numbers of residents that each caregiver contacts [5], aggressive testing and isolation, and sufficient PPE supplies. In addition, measures should be taken to incentivize high-risk members of the Austin workforce to remain at home during periods of community transmission.

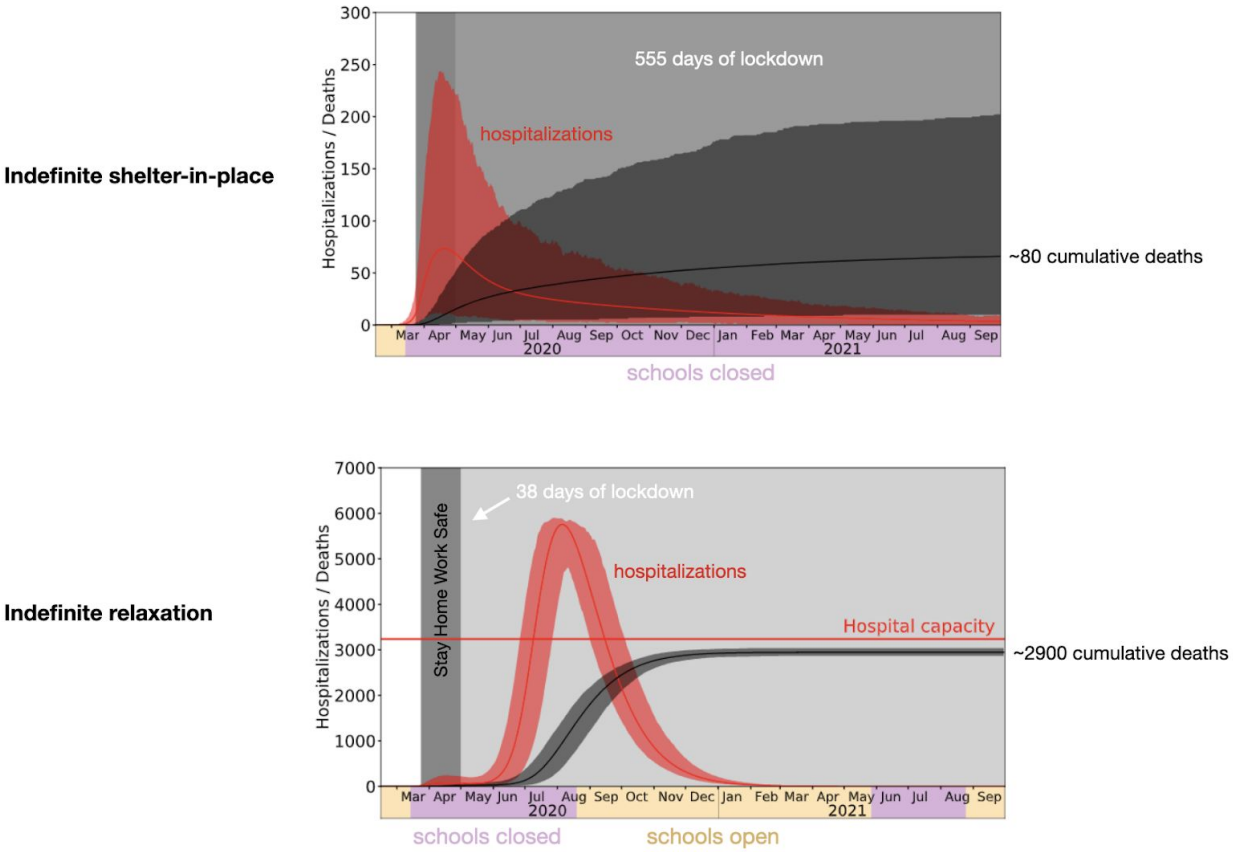

Figure 1. Projected COVID-19 hospitalizations and deaths in the Austin-Round Rock MSA from February 15 to September 30 17, 2021 under two extreme scenarios. The top graph shows a scenario in which strict social distancing is maintained through September 2021, resulting in a 90% reduction in transmission, along with vigilant cocooning of vulnerable populations (95% effective), and school closures. The bottom graph shows a scenario in which social distancing is permanently relaxed on May 1, 2020. Thereafter, transmission is reduced by only 40% (rather than 95%) by other precautions, such as extensive testing, contact tracing and isolation. Schools open in mid-August 2020 as scheduled and 95% effective cocooning of vulnerable populations is maintained through September 2021. In this scenario, hospitalizations are expected to grossly overrun capacity. The red curves indicate daily hospitalizations (heads in beds) and the black curves indicate cumulative deaths. The red horizontal line corresponds to the estimated local COVID-19 hospital surge capacity. Solid curves correspond to the point forecast and shaded regions are 90% prediction intervals based on 300 stochastic simulations. Yellow and pink shading along the bottom indicate periods where schools are open and closed, respectively.

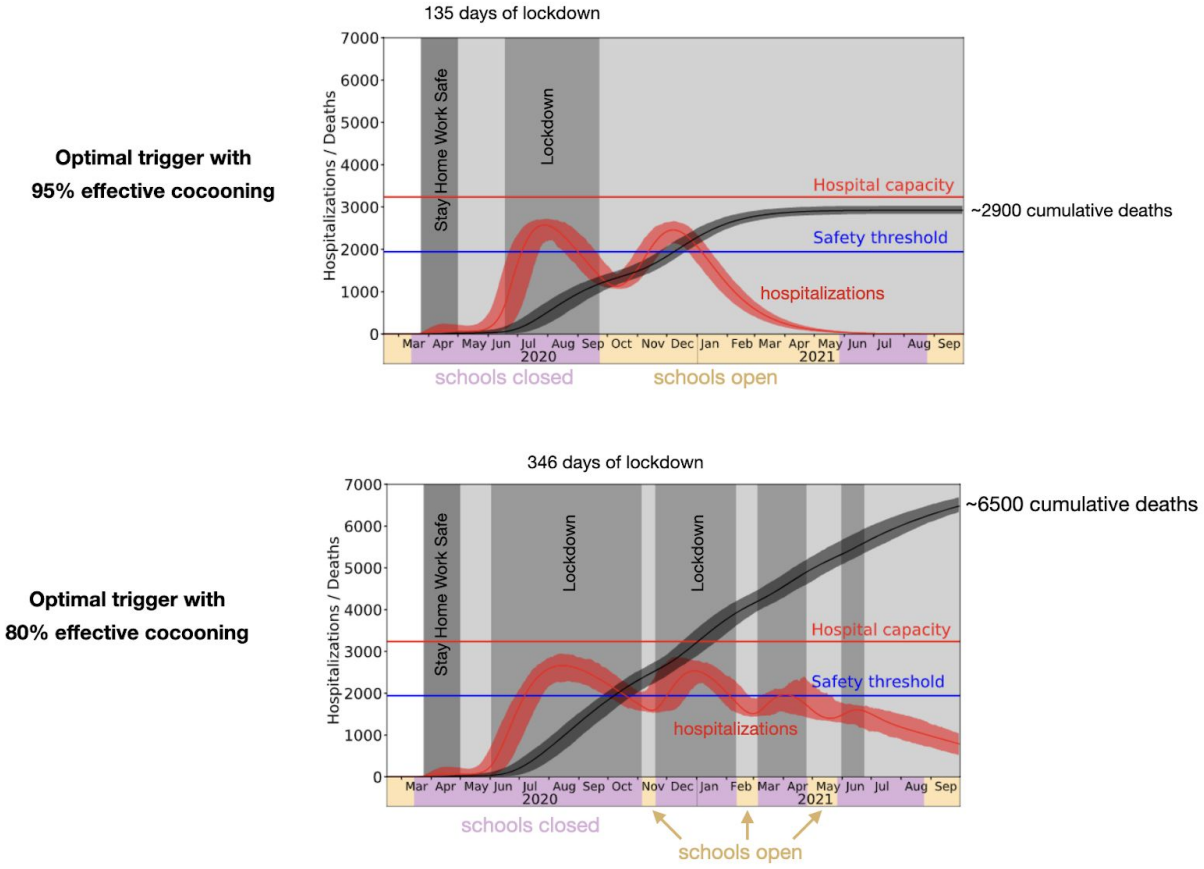

Figure 2. Projected COVID-19 hospitalizations and deaths in the Austin-Round Rock MSA from February 15 to September 30 17, 2021 under two optimized strategies for initiating and relaxing shelter-in-place (lockdown) orders. The top graph projects COVID-19 transmission under an adaptive lock-down strategy in which shelter-in-place orders are enacted when daily hospitalizations cross a specific threshold and relaxed when daily hospitalizations recede back below the threshold. This assumes 95% effective cocooning of vulnerable populations. The threshold used to trigger social distancing was optimized to minimize the days of lock-down while ensuring that hospital surges do not exceed capacity. The bottom graph shows an alternative scenario, in which cocooning of vulnerable populations is only 80% (rather than 95%) effective. Even under the optimal strategy for triggering lock-downs to avert catastrophic hospital surges, the expected deaths and days in lock-down both more than double, relative to cocooning at 95%. The red curves indicate daily hospitalizations (heads in beds) and the black curves indicate cumulative deaths. The red horizontal line corresponds to the estimated local COVID-19 hospital surge capacity. Solid curves correspond to the point forecast and shaded regions are 90% prediction intervals based on 300 stochastic simulations. Yellow and pink shading along the bottom indicate periods where schools are open and closed, respectively.

Appendix

COVID-19 Epidemic Model Structure and Parameters

The model structure is diagrammed in Figure A1 and described in the equations below.
For each age and risk group, we build a separate set of compartments to model the transitions between the states: susceptible (S), exposed (E), symptomatic infectious (I^Y), asymptomatic infectious (I^A), symptomatic infectious that are hospitalized (I^H), recovered (R), and deceased (D). The symbols S, E, I^Y, I^A, I^H, R, and D denote the number of people in that state in the given age/risk group and the total size of the age/risk group is $N = S + E + I^Y + I^A + I^H + R + D$. The model for individuals in age group a and risk group r is given by:

$$\frac{dS_{a,r}}{dt} = -\sum_{i\in A}\sum_{j\in K}(I^Y_{i,j}\omega^Y + I^A_{i,j}\omega^A + E_{i,j}\omega^E)(1-\kappa)\beta\phi_{a,i}/N_i$$

$$\frac{dE_{a,r}}{dt} = \sum_{i\in A}\sum_{j\in K}(I^Y_{i,j}\omega^Y + I^A_{i,j}\omega^A + E_{i,j}\omega^E)(1-\kappa)\beta\phi_{a,i}/N_i - \sigma E_{a,r}$$

$$\frac{dI^A_{a,r}}{dt} = (1-\tau)\sigma E_{a,r} - \gamma^A I^A_{a,r}$$

$$\frac{dI^Y_{a,r}}{dt} = \tau\sigma E_{a,r} - (1-\pi)\gamma^Y I^Y_{a,r} - \pi\eta I^Y_{a,r}$$

$$\frac{dI^H_{a,r}}{dt} = \pi\eta I^Y_{a,r} - (1-\nu)\gamma^H I^H_{a,r} - \nu\mu I^H_{a,r}$$

$$\frac{dR_{a,r}}{dt} = \gamma^A I^A_{a,r} + (1-\pi)\gamma^Y I^Y_{a,r} + (1-\nu)\gamma^H I^H_{a,r}$$

$$\frac{dD_{a,r}}{dt} = \nu\mu I^H_{a,r}$$

where A and K are all possible age and risk groups, ^{A}, ^{Y}, ^{H} are relative infectiousness of the I^A, I^Y, E compartments, respectively, β is transmission rate, κ is the transmission rate multiplier that models the reduction in transmission resulting from social distancing, $_{a,i}$ is the mixing rate between age group a, $i \in A$, ^{A}, ^{Y}, ^{H} are the recovery rates for the I^A, I^Y, I^H compartments, respectively, σ is the exposed rate, τ is the symptomatic ratio, π is the proportion of symptomatic individuals requiring hospitalization, η is rate at which hospitalized cases enter the hospital following symptom onset, ν is mortality rate for hospitalized cases, and μ is rate at which terminal patients die.

We model stochastic transitions between compartments using the τ-leap method [12,13] with key parameters given in Table S1. Assuming that the events at each time-step are independent and do not impact the underlying transition rates, the numbers of each type of event should follow Poisson distributions with means equal to the rate parameters. We thus simulate the model according to the following equations:

$$S_{a,r}(t+1) - S_{a,r}(t) = -P_1$$

$$E_{a,r}(t+1) - E_{a,r}(t) = P_1 - P_2$$

$$
\begin{aligned}
I^A_{a,r}(t+1) - I^A_{a,r}(t) &= (1-\tau)P_2 - P_3 \\
I^Y_{a,r}(t+1) - I^Y_{a,r}(t) &= \tau P_2 - P_4 - P_5 \\
I^H_{a,r}(t+1) - I^H_{a,r}(t) &= P_5 - P_6 - P_7 \\
R_{a,r}(t+1) - R_{a,r}(t) &= P_3 + P_4 + P_6 \\
D_{a,r}(t+1) - D_{a,r}(t) &= P_7,
\end{aligned}
$$

with

$$
\begin{aligned}
P_1 &\sim \text{Pois}(S_{a,r}(t)F_{a,r}(t)) \\
P_2 &\sim \text{Pois}(\sigma E_{a,r}(t)) \\
P_3 &\sim \text{Pois}(\gamma^A I^A_{a,r}(t)) \\
P_4 &\sim \text{Pois}((1-\pi)\gamma^Y I^Y_{a,r}(t)) \\
P_5 &\sim \text{Pois}(\pi\eta I^Y_{a,r}(t)) \\
P_6 &\sim \text{Pois}((1-\nu)\gamma^H I^H_a) \\
P_7 &\sim \text{Pois}(\nu\mu I^H_{a,r}(t))
\end{aligned}
$$

and where $F_{a,r}$ denotes the force of infection for individuals in age group a and risk group r and is given by:

$$
F_{a,r}(t) = \sum_{i\in A}\sum_{j\in K}(I^Y_{i,r}(t)\omega^Y + I^A_{i,r}(t)\omega^A + E_{i,j}(t)\omega^E)(1-\kappa)\beta_{a,i}\phi_{a,i}/N_i
$$

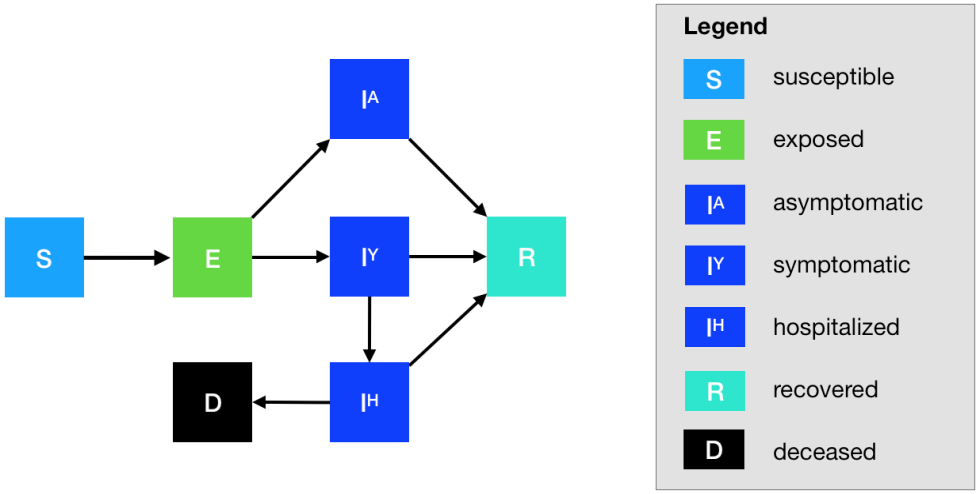

Figure A1. Compartmental model of COVID-19 transmission in a US city. Each subgroup (defined by age and risk) is modeled with a separate set of compartments. Upon infection, susceptible individuals (S) progress to exposed (E) and then to either symptomatic infectious (I^Y) or asymptomatic infectious (I^A). All asymptomatic cases eventually progress to a recovered class where they remain protected from future infection (R); symptomatic cases are either hospitalized (I^H) or recover. Mortality (D) varies by age group and risk group and is assumed to be preceded by hospitalization.

Estimating the effect of the Stay Home-Work Safe order

We estimated the transmission rate of COVID-19 in the Austin-Round Rock MSA before and after the March 24th *Stay Home-Work Safe* order using least-squares fitting, which compares the predicted and observed numbers of daily hospitalizations (i.e., heads in beds) for the Austin-Round Rock MSA. We assume that: (i) the epidemic starts with a single case on February 15, 2020 with an initial transmission rate of β, (ii) the transmission rate decreases when school closures are enacted on March 14, 2020 (by an amount determined by our pre-set contact matrices), (iii) the transmission rate decreases further by an amount d on March 25th following the *Stay Home-Work Safe* order.

We estimate β and d simultaneously using a nonlinear least squares fitting procedure in the SciPy/Python package [6]. For a given pair of β and d, we run a deterministic simulation of our model assuming central values for each parameter. Using a trust region method, the algorithm finds values of β and d that minimize the sum of squared daily differences between the simulated ($\hat{H}_t$) and actual (H_t) daily hospitalizations from March 13, 2020 through April 19, 2020: $S(\beta, d) = \sum_t (H_t - \hat{H}_t)^2$.

We calculated 95% confidence intervals for the social distancing parameter indirectly by running 500 stochastic simulations for each of the following possible values of d': 0.0, 0.05, ..., 0.95, 1.0. For each value of d', we conducted the following analysis to determine if d' lies inside the 95% confidence interval for d.

- For all simulations, we calculate the day-to-day difference in hospitalizations (i.e., heads in beds) during the period following the *Stay Home-Work Safe* order: $\hat{z}_t = \hat{H}_t - \hat{H}_{t-1}$. We do the same for the actual data: $z_t = H_t - H_{t-1}$.

- We compute the 95% prediction interval for $\hat{z}_t$ across all 500 stochastic simulations for d' for each day t .

- We then conduct a test of the null hypothesis $H_0 : d' = d$. Under this null hypothesis, we would expect roughly 95% of the observed data (z_t) to fall within the 95% prediction band for $\hat{z}_t$ that we constructed from our simulations. By analyzing the day-to-day difference in hospitalizations rather than daily hospitalizations, we can assume that the data are independent from one day to the next. Then the expected number of observed values contained in the 95% prediction band is given by the binomial expression:

  $$N_{\text{contained}} \sim B\left(N_{\text{points}}, 0.95\right)$$

  where $N_{\text{contained}}$ is the number of data points contained within the 95% prediction band and N_{points} is the total number of data points (i.e., days).

- If the binomial probability of $N_{\text{contained}}$ is less than 0.05, we reject the null hypothesis $H_0 : d' = d$

To construct a 95% confidence interval for d we take the minimum and maximum d' for which we did not reject the null hypothesis $H_0 : d' = d$.

Table A1. Initial conditions, school closures and social distancing policies

Variable	Settings
Initial day of simulation	2/15/2020
Initial infection number in locations	1 symptomatic case in 18-49y age group
School closure	3/15/2020 - 8/17/2020
Age-specific and day-specific contact rates	Home, work, other and school matrices provided in Tables S4.1-S4.4, and are modified to reflect school closures and other changes in contact patterns and transmission rates during simulations

Table A2. Model parameters[a]

Parameters	Best guess values (doubling time = 4 days)	Source
β: baseline transmission rate	0.035	Fitted to daily COVID-19 hospitalizations in Austin-Round Rock MSA
κ: reduction in transmission	From 2020-02-15 to 2020-03-24: 0 From 2020-03-25 to 2020-05-01: 0.95 [95% CI: 0.7 - 1] After 2020-05-01: Depends on scenario	From 2020-03-25 to 2020-05-01: fitted to daily COVID-19 hospitalizations in Austin-Round Rock MSA
γ^A: recovery rate on asymptomatic compartment	Equal to γ^Y	
γ^Y: recovery rate on symptomatic non-treated compartment	$\frac{1}{\gamma^Y} \sim \text{Triangular}(21.2, 22.6, 24.4)$	Verity et al. [7]
τ: symptomatic proportion (%)	82.1	Mizumoto et al.[3]
σ: exposed rate	$\frac{1}{\sigma} \sim \text{Triangular}(5.6, 7, 8.2)$	Lauer et al.[2]
P: proportion of	12.6	Du et al.[8]

pre-symptomatic transmission (%)		
ω^E: relative infectiousness of infectious individuals in compartment E	$\omega^E = \frac{(\frac{YHR}{\eta} + \frac{1-YHR}{\gamma^Y})\omega^Y \sigma P}{1-P}$	
ω^A: relative infectiousness of infectious individuals in compartment I^A	0.4653	Set to mean of ω^E
IFR: infected fatality ratio, age specific (%)	Low risk: [0.0009, 0.0022, 0.0339, 0.2520, 0.6440] High risk: [0.0092, 0.0218, 0.3388, 2.5197, 6.4402]	Age adjusted from Verity et al. [7]
YFR: symptomatic fatality ratio, age specific (%)	Low risk: [0.0011165, 0.0027 , 0.0412, 0.3069, 0.7844] High risk: [0.0112, 0.0265, 0.4126, 3.0690, 7.8443]	$YFR = \frac{IFR}{1-\tau}$
h: high-risk proportion, age specific (%)	[8.2825, 14.1121, 16.5298, 32.9912, 47.0568]	Estimated using 2015-2016 Behavioral Risk Factor Surveillance System (BRFSS) data with multilevel regression and poststratification using CDC's list of conditions that may increase the risk of serious complications from influenza[9–11]

[a]Values given as five-element vectors are age-stratified with values corresponding to 0-4, 5-17, 18-49, 50-64, 65+ year age groups, respectively.

Table A3 Hospitalization parameters

Parameters	Value	Source
γ^H: recovery rate in hospitalized compartment	1/14	14 day-average from admission to discharge (UT Austin Dell Med)
YHR: symptomatic case hospitalization rate (%)	Low risk: [0.0279, 0.0215, 1.3215, 2.8563, 3.3873] High risk: [0.2791, 0.2146, 13.2154, 28.5634, 33.8733]	Age adjusted from Verity et al. [7]
π: rate of symptomatic individuals go to hospital, age-specific	$\pi = \frac{\gamma^Y * YHR}{\eta + (\gamma^Y - \eta)YHR}$	
η: rate from symptom onset to hospitalized	0.1695	5.9 day average from symptom onset to hospital admission Tindale et al.[12]

μ: rate from hospitalized to death	1/14	14 day-average from admission to death (UT Austin Dell Med)
HFR: hospitalized fatality ratio, age specific (%)	[4, 12.365, 3.122, 10.745, 23.158]	$HFR = \frac{IFR}{YHR(1-\tau)}$
ν: death rate on hospitalized individuals, age specific	[0.0390, 0.1208, 0.0304, 0.1049, 0.2269]	$\nu = \frac{\gamma^H HFR}{\mu + (\gamma^H - \mu)HFR}$
ICU: proportion hospitalized people in ICU	[0.15, 0.20, 0.15, 0.20, 0.15]	CDC planning scenarios (based on US seasonal flu data)
Vent: proportion of individuals in ICU needing ventilation	$[\frac{2}{3}, \frac{2}{3}, \frac{2}{3}, \frac{2}{3}, \frac{2}{3}]$	Assumption
d_{ICU} : duration of stay in ICU	10 days	Assumption, set equal to duration of ventilation
d_V : duration of ventilation	10 days	Assumption
Healthcare capacity	Hospital bed: 4299 (assume 80% available for COVID-19) ICU bed: 755 (90% available) Ventilator: 755 (90% available)	Estimates provided by each of the region's hospital systems and aggregated by regional public health leaders

Table A4.1 Home contact matrix. Daily number contacts by age group at home.

	0-4y	**5-17y**	**18-49y**	**50-64y**	**65y+**
0-4y	0.5	0.9	2.0	0.1	0.0
5-17y	0.2	1.7	1.9	0.2	0.0
18-49y	0.2	0.9	1.7	0.2	0.0
50-64y	0.2	0.7	1.2	1.0	0.1
65y+	0.1	0.7	1.0	0.3	0.6

Table A4.2 School contact matrix. Daily number contacts by age group at school.

	0-4y	**5-17y**	**18-49y**	**50-64y**	**65y+**
0-4y	1.0	0.5	0.4	0.1	0.0
5-17y	0.2	3.7	0.9	0.1	0.0
18-49y	0.0	0.7	0.8	0.0	0.0
50-64y	0.1	0.8	0.5	0.1	0.0
65y+	0.0	0.0	0.1	0.0	0.0

Table A4.3 Work contact matrix. Daily number contacts by age group at work.

	0-4y	5-17y	18-49y	50-64y	65y+
0-4y	0.0	0.0	0.0	0.0	0.0
5-17y	0.0	0.1	0.4	0.0	0.0
18-49y	0.0	0.2	4.5	0.8	0.0
50-64y	0.0	0.1	2.8	0.9	0.0
65y+	0.0	0.0	0.1	0.0	0.0

Table A4.4 Others contact matrix. Daily number contacts by age group at other locations.

	0-4y	5-17y	18-49y	50-64y	65y+
0-4y	0.7	0.7	1.8	0.6	0.3
5-17y	0.2	2.6	2.1	0.4	0.2
18-49y	0.1	0.7	3.3	0.6	0.2
50-64y	0.1	0.3	2.2	1.1	0.4
65y+	0.0	0.2	1.3	0.8	0.6

Estimation of age-stratified proportion of population at high-risk for COVID-10 complications

We estimate age-specific proportions of the population at high risk of complications from COVID-19 based on data for Austin, TX and Round-Rock, TX from the CDC's 500 cities project (Figure A2).[13] We assume that high risk conditions for COVID-19 are the same as those specified for influenza by the CDC.[9] The CDC's 500 cities project provides city-specific estimates of prevalence for several of these conditions among adults.[14] The estimates were obtained from the 2015-2016 Behavioral Risk Factor Surveillance System (BRFSS) data using a small-area estimation methodology called multi-level regression and poststratification.[10,11] It links geocoded health surveys to high spatial resolution population demographic and socioeconomic data.[11]

Estimating high-risk proportions for adults. To estimate the proportion of adults at high risk for complications, we use the CDC's 500 cities data, as well as data on the prevalence of HIV/AIDS, obesity and pregnancy among adults (Table A6).

The CDC 500 cities dataset includes the prevalence of each condition on its own, rather than the prevalence of multiple conditions (e.g., dyads or triads). Thus, we use separate co-morbidity estimates to determine overlap. Reference about chronic conditions[15] gives US estimates for the proportion of the adult population with 0, 1 or 2+ chronic conditions, per age group. Using

this and the 500 cities data we can estimate the proportion of the population p_{HR} in each age group in each city with at least one chronic condition listed in the CDC 500 cities data (Table A6) putting them at high-risk for flu complications.

HIV: We use the data from table 20a in CDC HIV surveillance report[16] to estimate the population in each risk group living with HIV in the US (last column, 2015 data). Assuming independence between HIV and other chronic conditions, we increase the proportion of the population at high-risk for influenza to account for individuals with HIV but no other underlying conditions.
Morbid obesity: A BMI over 40kg/m^2 indicates morbid obesity, and is considered high risk for influenza. The 500 Cities Project reports the prevalence of obese people in each city with BMI over 30kg/m^2 (not necessarily morbid obesity). We use the data from table 1 in Sturm and Hattori[17] to estimate the proportion of people with BMI>30 that actually have BMI>40 (across the US); we then apply this to the 500 Cities obesity data to estimate the proportion of people who are morbidly obese in each city. Table 1 of Morgan et al.[18] suggests that 51.2% of morbidly obese adults have at least one other high risk chronic condition, and update our high-risk population estimates accordingly to account for overlap.
Pregnancy: We separately estimate the number of pregnant women in each age group and each city, following the methodology in CDC reproductive health report.[19] We assume independence between any of the high-risk factors and pregnancy, and further assume that half the population are women.

Estimating high-risk proportions for children. Since the 500 Cities Project only reports data for adults 18 years and older, we take a different approach to estimating the proportion of children at high risk for severe influenza. The two most prevalent risk factors for children are asthma and obesity; we also account for childhood diabetes, HIV and cancer.
From Miller et al.[20], we obtain national estimates of chronic conditions in children. For asthma, we assume that variation among cities will be similar for children and adults. Thus, we use the relative prevalences of asthma in adults to scale our estimates for children in each city. The prevalence of HIV and cancer in children are taken from CDC HIV surveillance report[16] and cancer research report,[21] respectively.

We first estimate the proportion of children having either asthma, diabetes, cancer or HIV (assuming no overlap in these conditions). We estimate city-level morbid obesity in children using the estimated morbid obesity in adults multiplied by a national constant ratio for each age group estimated from Hales et al.,[22] this ratio represents the prevalence in morbid obesity in children given the one observed in adults. From Morgan et al.,[18] we estimate that 25% of morbidly obese children have another high-risk condition and adjust our final estimates accordingly.

Resulting estimates. We compare our estimates for the Austin-Round Rock Metropolitan Area to published national-level estimates[23] of the proportion of each age group with underlying high risk conditions (Table A6). The biggest difference is observed in older adults, with Austin

having a lower proportion at risk for complications for COVID-19 than the national average; for 25-39 year olds the high risk proportion is slightly higher than the national average.

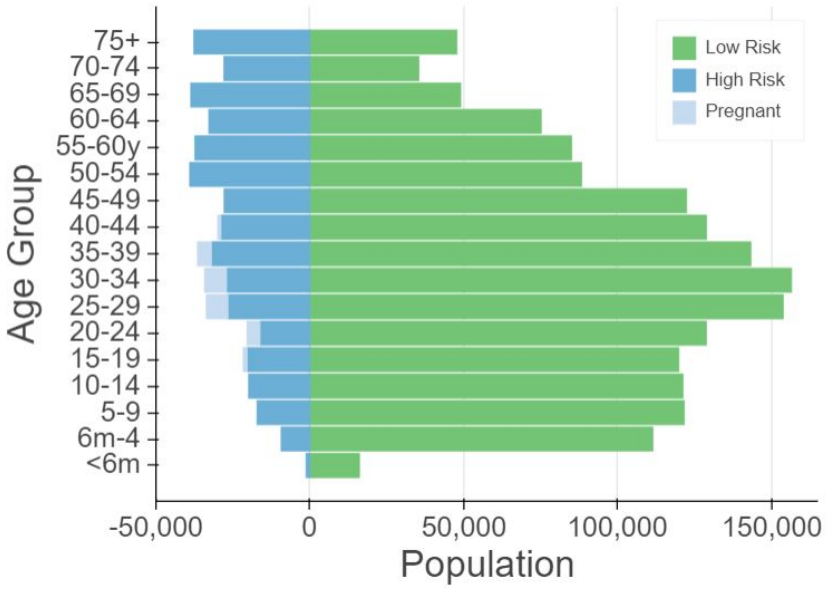

Figure A2. Demographic and risk composition of the Austin-Round Rock MSA. Bars indicate age-specific population sizes, separated by low risk, high risk, and pregnant. High risk is defined as individuals with cancer, chronic kidney disease, COPD, heart disease, stroke, asthma, diabetes, HIV/AIDS, and morbid obesity, as estimated from the CDC 500 Cities Project,[13] reported HIV prevalence[16] and reported morbid obesity prevalence,[17,18] corrected for multiple conditions. The population of pregnant women is derived using the CDC's method combining fertility, abortion and fetal loss rates.[24–26]

Table A6. High-risk conditions for influenza and data sources for prevalence estimation

Condition	Data source
Cancer (except skin), chronic kidney disease, COPD, coronary heart disease, stroke, asthma, diabetes	CDC 500 cities [13]
HIV/AIDS	CDC HIV Surveillance report [16]
Obesity	CDC 500 cities [13], Sturm and Hattori [17], Morgan et al.[18]
Pregnancy	National Vital Statistics Reports [24] and abortion data [25]

Table A7: Comparison between published national estimates and Austin-Round Rock MSA estimates of the percent of the population at high-risk of influenza/COVID-19 complications.

Age Group	National estimates [22]	Austin (excluding pregnancy)	Pregnant women (proportion of age group)
0 to 6 months	NA	6.8	-
6 months to 4 years	6.8	7.4	-
5 to 9 years	11.7	11.6	-
10 to 14 years	11.7	13.0	-
15 to 19 years	11.8	13.3	1.7
20 to 24 years	12.4	10.3	5.1
25 to 34 years	15.7	13.5	7.8
35 to 39 years	15.7	17.0	5.1
40 to 44 years	15.7	17.4	1.2
45 to 49 years	15.7	17.7	-
50 to 54 years	30.6	29.6	-
55 to 60 years	30.6	29.5	-
60 to 64 years	30.6	29.3	-
65 to 69 years	47.0	42.2	-
70 to 74 years	47.0	42.2	-
75 years and older	47.0	42.2	-

References

1. Calendar of Events. In: Austin ISD [Internet]. [cited 26 Mar 2020]. Available: https://www.austinisd.org/calendar

2. Lauer SA, Grantz KH, Bi Q, Jones FK, Zheng Q, Meredith HR, et al. The Incubation Period of Coronavirus Disease 2019 (COVID-19) From Publicly Reported Confirmed Cases: Estimation and Application. Ann Intern Med. 2020. doi:10.7326/M20-0504

3. Mizumoto K, Kagaya K, Zarebski A, Chowell G. Estimating the Asymptomatic Proportion of 2019 Novel Coronavirus onboard the Princess Cruises Ship, 2020. Infectious Diseases (except HIV/AIDS). medRxiv; 2020. doi:10.1101/2020.02.20.20025866

4. Keeling MJ, Rohani P. Modeling Infectious Diseases in Humans and Animals. Princeton University Press; 2011. Available: https://play.google.com/store/books/details?id=LxzILSuKDhUC

5. Gillespie DT. Approximate accelerated stochastic simulation of chemically reacting systems. J Chem Phys. 2001;115: 1716–1733. doi:10.1063/1.1378322

6. minimize(method='trust-constr') — SciPy v1.4.1 Reference Guide. [cited 19 Apr 2020]. Available: https://docs.scipy.org/doc/scipy/reference/optimize.minimize-trustconstr.html

7. Verity R, Okell LC, Dorigatti I, Winskill P, Whittaker C, Imai N, et al. Estimates of the severity of COVID-19 disease. Epidemiology. medRxiv; 2020. doi:10.1101/2020.03.09.20033357

8. Du Z, Xu X, Wu Y, Wang L, Cowling BJ, Meyers LA. The serial interval of COVID-19 from publicly reported confirmed cases. Epidemiology. medRxiv; 2020. doi:10.1101/2020.02.19.20025452

9. CDC. People at High Risk of Flu. In: Centers for Disease Control and Prevention [Internet]. 1 Nov 2019 [cited 26 Mar 2020]. Available: https://www.cdc.gov/flu/highrisk/index.htm

10. CDC - BRFSS. 5 Nov 2019 [cited 26 Mar 2020]. Available: https://www.cdc.gov/brfss/index.html

11. Zhang X, Holt JB, Lu H, Wheaton AG, Ford ES, Greenlund KJ, et al. Multilevel regression and poststratification for small-area estimation of population health outcomes: a case study of chronic obstructive pulmonary disease prevalence using the behavioral risk factor surveillance system. Am J Epidemiol. 2014;179: 1025–1033. doi:10.1093/aje/kwu018

12. Tindale L, Coombe M, Stockdale JE, Garlock E, Lau WYV, Saraswat M, et al. Transmission interval estimates suggest pre-symptomatic spread of COVID-19. Epidemiology. medRxiv; 2020. doi:10.1101/2020.03.03.20029983

13. 500 Cities Project: Local data for better health | Home page | CDC. 5 Dec 2019 [cited 19 Mar 2020]. Available: https://www.cdc.gov/500cities/index.htm

14. Health Outcomes | 500 Cities. 25 Apr 2019 [cited 28 Mar 2020]. Available: https://www.cdc.gov/500cities/definitions/health-outcomes.htm

15. Part One: Who Lives with Chronic Conditions. In: Pew Research Center: Internet, Science & Tech [Internet]. 26 Nov 2013 [cited 23 Nov 2019]. Available: https://www.pewresearch.org/internet/2013/11/26/part-one-who-lives-with-chronic-conditions/

16. for Disease Control C, Prevention, Others. HIV surveillance report. 2016; 28. URL: http://www cdc gov/hiv/library/reports/hiv-surveil-lance html Published November. 2017.

17. Sturm R, Hattori A. Morbid obesity rates continue to rise rapidly in the United States. Int J Obes . 2013;37: 889–891. doi:10.1038/ijo.2012.159

18. Morgan OW, Bramley A, Fowlkes A, Freedman DS, Taylor TH, Gargiullo P, et al. Morbid

obesity as a risk factor for hospitalization and death due to 2009 pandemic influenza A(H1N1) disease. PLoS One. 2010;5: e9694. doi:10.1371/journal.pone.0009694

19. Estimating the Number of Pregnant Women in a Geographic Area from CDC Division of Reproductive Health. Available: https://www.cdc.gov/reproductivehealth/emergency/pdfs/PregnacyEstimatoBrochure508.pdf

20. Miller GF, Coffield E, Leroy Z, Wallin R. Prevalence and Costs of Five Chronic Conditions in Children. J Sch Nurs. 2016;32: 357–364. doi:10.1177/1059840516641190

21. Cancer Facts & Figures 2014. [cited 30 Mar 2020]. Available: https://www.cancer.org/research/cancer-facts-statistics/all-cancer-facts-figures/cancer-facts-figures-2014.html

22. Hales CM, Fryar CD, Carroll MD, Freedman DS, Ogden CL. Trends in Obesity and Severe Obesity Prevalence in US Youth and Adults by Sex and Age, 2007-2008 to 2015-2016. JAMA. 2018;319: 1723–1725. doi:10.1001/jama.2018.3060

23. Zimmerman RK, Lauderdale DS, Tan SM, Wagener DK. Prevalence of high-risk indications for influenza vaccine varies by age, race, and income. Vaccine. 2010;28: 6470–6477. doi:10.1016/j.vaccine.2010.07.037

24. Martin JA, Hamilton BE, Osterman MJK, Driscoll AK, Drake P. Births: Final Data for 2017. Natl Vital Stat Rep. 2018;67: 1–50. Available: https://www.ncbi.nlm.nih.gov/pubmed/30707672

25. Jatlaoui TC, Boutot ME, Mandel MG, Whiteman MK, Ti A, Petersen E, et al. Abortion Surveillance - United States, 2015. MMWR Surveill Summ. 2018;67: 1–45. doi:10.15585/mmwr.ss6713a1

26. Ventura SJ, Curtin SC, Abma JC, Henshaw SK. Estimated pregnancy rates and rates of pregnancy outcomes for the United States, 1990-2008. Natl Vital Stat Rep. 2012;60: 1–21. Available: https://www.ncbi.nlm.nih.gov/pubmed/22970648